Four-compartment epidemic model with retarded transition rates

Téo Granger,[1] Thomas M. Michelitsch,[1,*] Michael Bestehorn,[2] Alejandro P. Riascos,[3] and Bernard A. Collet[1]
[1]*Sorbonne Université, Institut Jean le Rond d'Alembert, CNRS UMR 7190, 4 Place Jussieu, 75252 Paris Cedex 05, France*
[2]*Institut für Physik, Brandenburgische Technische Universität Cottbus-Senftenberg, Erich-Weinert-Straße 1, 03046 Cottbus, Germany*
[3]*Instituto de Física, Universidad Nacional Autónoma de México, Apartado Postal 20-364, 01000 Ciudad de México, Mexico*

(Received 21 November 2022; accepted 17 March 2023; published 18 April 2023)

We study an epidemic model for a constant population by taking into account four compartments of the individuals characterizing their states of health. Each individual is in one of the following compartments: susceptible S; incubated, i.e., infected yet not infectious, C; infected and infectious I; and recovered, i.e., immune, R. An infection is visible only when an individual is in state I. Upon infection, an individual performs the transition pathway $S \to C \to I \to R \to S$, remaining in compartments C, I, and R for a certain random waiting time t_C, t_I, and t_R, respectively. The waiting times for each compartment are independent and drawn from specific probability density functions (PDFs) introducing memory into the model. The first part of the paper is devoted to the macroscopic *S-C-I-R-S* model. We derive memory evolution equations involving convolutions (time derivatives of general fractional type). We consider several cases. The memoryless case is represented by exponentially distributed waiting times. Cases of long waiting times with fat-tailed waiting-time distributions are considered as well where the *S-C-I-R-S* evolution equations take the form of time-fractional ordinary differential equations. We obtain formulas for the endemic equilibrium and a condition of its existence for cases when the waiting-time PDFs have existing means. We analyze the stability of healthy and endemic equilibria and derive conditions for which the endemic state becomes oscillatory (Hopf) unstable. In the second part, we implement a simple multiple-random-walker approach (microscopic model of Brownian motion of Z independent walkers) with random *S-C-I-R-S* waiting times in computer simulations. Infections occur with a certain probability by collisions of walkers in compartments I and S. We compare the endemic states predicted in the macroscopic model with the numerical results of the simulations and find accordance of high accuracy. We conclude that a simple random-walker approach offers an appropriate microscopic description for the macroscopic model. The *S-C-I-R-S*–type models open a wide field of applications allowing the identification of pertinent parameters governing the phenomenology of epidemic dynamics such as extinction, convergence to a stable endemic equilibrium, or persistent oscillatory behavior.

DOI: 10.1103/PhysRevE.107.044207

I. INTRODUCTION

The origin of modern epidemic modeling started with the seminal work of Kermack and McKendrick almost a century ago [1]. They introduced the so-called susceptible-infected-recovered (SIR) model, where SIR stands for three compartments characterizing the states of health of an individual, namely, S denotes susceptible, I infected, and R recovered. The classical SIR model and various generalizations are able to capture some of the features of epidemic spreading of infectious diseases as observed in influenza, measles, mumps, and rubella. In the meantime, a huge burst of compartment models and generalizations of the SIR model have been introduced [2,3].

While the interest in mathematical modeling of epidemic spreading was growing continuously, it is unsurprising that the emergence of the COVID pandemic has launched an enhanced interest and urgent need in advanced epidemic modeling [4]. Many models consider a set of nonlinear ordinary differential equations (ODEs) for the time evolution of the compartment populations where a new direction is about to emerge by combining these models with approaches inspired by network science [5–11] and fractional dynamics [12–16].

It has turned out that in many cases epidemics including COVID exhibit quasiperiodic patterns and spontaneous new outbreaks even after longer times of inactivity. Persistent oscillatory characteristics in epidemic dynamics had already been pointed out a long time ago in the work of Soper [17]. Indeed, a major drawback of classical SIR-type models without memory effects lies in their incapacity to capture (persistent) oscillatory behavior.

The present paper aims to tackle this issue and is a generalization of recent works [10,11]. Reference [11] introduced a SIRS compartment model which takes into account a random duration of immunity (recovered) R allowing a delayed transition $R \to S$. What is found is that this model is able to capture persistent oscillatory behavior in the number of infected individuals. This feature appears as oscillatory Hopf instability of the endemic state. In the first part of our paper we extend this model to four compartments as relevant states of health in order to capture a larger variety of epidemics. We consider the four following compartments: S, susceptible; C,

*Corresponding author: thomas.michelitsch@sorbonne-universite.fr

infected but not yet infectious (in the incubation phase); I, infected and infectious (ill); and R, recovered and immune. We assume random sojourn times (waiting times) t_C, t_I, and t_R an individual once infected spends in each of the compartments C, I, and R. The sojourn time t_C in compartment C is interpreted as incubation time, i.e., the delay between infection and the outbreak of the disease. The sojourn time t_I is the duration of the disease (infected and infectious state) and t_R indicates the immunity period after recovery. It appears natural to assume that these variables are not fixed constants but individually fluctuating random variables drawn by specific distributions. With these assumptions, we derive the *S-C-I-R-S* evolution equations where we focus on several pertinent situations of waiting times with existing and nonexisting mean. For waiting-time probability density functions (PDFs) with an existing mean, we derive explicit formulas for the endemic equilibrium and analyze its stability.

In the second part of the paper we combine our *S-C-I-R-S* model with a multiple-random-walker approach which is implemented in computer simulations. We present a case study and give numerical evidence that a simple random-walk approach (Brownian motion) offers an appropriate description of the *S-C-I-R-S* dynamics with memory.

Indeed, the uncertainty in the available data (for instance, the number of infected individuals) in many real-world epidemics is a major problem which strongly affects their predictability. Therefore, stochastic approaches which include hypotheses on randomness of the involved quantities, for instance, on the allowed steps in a random walk of the individuals or in the model parameters (such as waiting times in the compartments or considering the transition rates as random variables), offer powerful modeling tools dealing in a natural way with the lack of available information. A stochastic approach with random transition rates has been presented in a recent work of Faranda *et al.* [18] to model the second wave of COVID. In that model the epidemic dynamics was described in the framework of a stochastic susceptible-exposed-infected-recovered compartment model with classical types of evolution equations where the transition rates are random variables drawn from a Gaussian distribution. In that work the compartment R accounts for the recovered (immune) and dead individuals where immunity is never-ending (infinite immunity time). Hence there is no transition back to the susceptible state. The compartment E (exposed) corresponds to infected but not infectious individuals. As a consequence of the infinite immunity time, the endemic state is stable and (in contrast to our *S-C-I-R-S* model) no persistent oscillations in the number of infections occur in their model. We discuss cases of infinite waiting times in the compartments in our model as a limiting case of infinite immunity duration (see Sec. II E) where a stable endemic state with a constant population of individuals in compartment R in the limit of large times occurs, consistent with their result [18].

II. FOUR-COMPARTMENT MODEL

A. Basic notions

We consider a constant (time-independent) total population of $Z = Z_S + Z_C + Z_I + Z_R$ individuals (random walkers) where $Z_S(t)$, $Z_C(t)$, $Z_I(t)$, and $Z_R(t)$ indicate their numbers in the compartments S, C, I, and R at time t. Assuming a constant total population means that we focus here on the large class of epidemics for which the mortality as well as natural birth and death processes can be neglected, at least on relevant timescales of the epidemic dynamics, for instance, during the occurrence of infection waves. More precisely, we assume that the waiting times $t_{C,I,R}$ are small compared to the expected lifetimes of the individuals. We consider here a continuous-time model for $Z \gg 1$ walkers with the compartment population fractions $s(t) = \frac{Z_S(t)}{Z}$, $c(t) = \frac{Z_C(t)}{Z}$, $j(t) = \frac{Z_I(t)}{Z}$, and $r(t) = \frac{Z_R(t)}{Z}$. We allow for each walker the following transition pathway: $S \to C \to I \to R \to S$. Intuitively, we infer that allowing for persistent oscillatory and (quasi)periodic behavior, it is necessary to have a closed (cyclic) pathway $S \to \cdots \to S$ of transitions in a constant (time-independent) total population as assumed in our model. However, this is no longer true in models where the total population is allowed to vary, such as considered in the article of Manfredi and Salinelli [19]. They demonstrated in that work that sustained oscillations may occur when being induced in an exponentially growing total population. We assume that $t_C, t_I, t_R \geqslant 0$ are mutually *independent* random waiting times an individual spends (after infection) in the compartments C, I, and R drawn from specific PDFs, which we denote by the kernels $K_C(t)$, $K_I(t)$, and $K_R(t)$, respectively. These kernels have to be causal functions[1] with, for instance,

$$\mathrm{Prob}(t_C \in [\tau, \tau + d\tau]) = K_C(\tau)d\tau, \quad t_C > 0,$$

which indicates the probability that the incubation time $t_C \in [\tau, \tau + d\tau]$, which is clearly nonzero only for $\tau \geqslant 0$ as $t_C \geqslant 0$. In other words, given a walker has entered compartment C at $\tau = 0$, then $K_C(\tau)d\tau$ indicates the probability that this walker leaves compartment C during the infinitesimal interval $[\tau, \tau + d\tau]$ (by a transition $C \to I$). We introduce the infection rate $\mathcal{A}(t) = \mathcal{A}(j(t), s(t), t) \geqslant 0$ (number of infections per walker and unit time or entry rate to the incubated compartment C at time t having units of s^{-1}). We point out that $\mathcal{A}(t)$ is not a known given function of time t but rather an implicit nonlinear function of $s(t)$ and $j(t)$, namely, $\mathcal{A}(t) = \mathcal{A}(s(t), j(t))$. This quantity contains macroscopic information on the instantaneous number of collisions of individuals in the reactive compartments S and I and needs to be specified by model assumptions. It is important to point out that $\mathcal{A}(t)$ does not depend on the fractions $c(t)$ and $r(t)$ of the invisible compartments C and R.

We assume here the most simple nonlinear form $\mathcal{A}(t) = \beta j(t)s(t)$, where $\beta > 0$ is a constant independent of time where β^{-1} introduces a characteristic timescale. In addition, β is also a macroscopic measure for the infection probability in a collision of an S and an I walker. The microscopic picture which we will invoke subsequently and implement in computer simulations indeed is that the infection rate is driven by random collisions between infected and susceptible independent random walkers.

[1] A function $g(t)$ is called causal if $g(t) = 0$ for $t < 0$, i.e., nonzero only for $t \geqslant 0$.

With these simple assumptions, we can establish model equations governing the time evolution of the fractions $s(t)$, $c(t)$, $j(t)$, and $r(t)$. We consider the dynamics starting at time $t = 0$ with an initial condition $s(0) = 1 - j_0$ and $j(0) = j_0$ (many healthy and a few infected walkers) and no incubated or recovered walkers $c(0) = r(0) = 0$. Our (*S-C-I-R-S*)- model evolution equations have the general structure

$$\frac{d}{dt}s(t) = -\mathcal{A}(t) + (\mathcal{A} \star K_C \star K_I \star K_R)(t), \tag{1a}$$

$$\frac{d}{dt}c(t) = \mathcal{A}(t) - (\mathcal{A} \star K_C)(t), \tag{1b}$$

$$\frac{d}{dt}j(t) = (\mathcal{A} \star K_C)(t) - (\mathcal{A} \star K_C \star K_I)(t), \tag{1c}$$

$$\frac{d}{dt}r(t) = (\mathcal{A} \star K_C \star K_I)(t) - (\mathcal{A} \star K_C \star K_I \star K_R)(t). \tag{1d}$$

The sum of these rates is vanishing due to $s(t) + c(t) + j(t) + r(t) = 1$. In order for an epidemic to start, it is necessary that the globally healthy state becomes unstable when the initial state is close to the healthy state with $j_0 \sim \frac{1}{Z} \to 0+$, i.e., where, for instance, only one infected walker is present at $t = 0$ (among a large population Z). We analyze the stability of the healthy state subsequently in detail. In (1) we have employed the notation

$$(K \star f)(t) = \int_0^t K(t-\tau) f(\tau) d\tau, \quad t \geqslant 0 \tag{2}$$

for convolutions of causal functions $K(t)$ and $f(t)$. Be aware that convolutions commute and are associative, which can be seen by the representation ($t \geqslant 0$) of the multiple convolution

$$\begin{aligned}(K_1 \star K_2 \star \cdots \star K_n)(t) =: & \int_{-\infty}^{\infty} \cdots \int_{-\infty}^{\infty} d\tau_1 \cdots d\tau_n \\ & \times \delta(t - \tau_1 - \cdots - \tau_n) \\ & \times K_1(\tau_1) \cdots K_n(\tau_n),\end{aligned} \tag{3}$$

where $\delta(\cdots)$ indicates the Dirac δ function and (3) is nonzero only for $t \geqslant 0$ [causality of the $K_i(\tau)$]. We introduce the Laplace transform of our kernels, which we define as

$$\hat{K}(\lambda) = \int_0^{\infty} e^{-\lambda t} K(t) dt,$$

where λ indicates the Laplace variable and $\hat{K}(\lambda)|_{\lambda=0} = 1$ indicates that the kernels are normalized PDFs. A further observation is worth mentioning. Any (multiple) convolution of PDFs gives again a PDF. This can be easily seen by integrating (3) over time to yield one. Therefore, the kernels $K_C(t)$, $(K_C \star K_I)(t)$, and $(K_C \star K_I \star K_R)(t)$ which appear in (1) all are (normalized and causal) PDFs representing the densities of the random variables t_C, $t_C + t_I$, and $t_C + t_I + t_R$, respectively. We can see in (1) that for each compartment where an individual remains for a random duration, an additional convolution occurs describing the delayed transition out of the compartment. These delayed transitions introduce memory into the rates of individuals leaving the compartments. We will give a careful account of this issue later [subsequent representation (11)].

The interpretation of (1) is as follows. In Eq. (1a) $\mathcal{A}(t)$ is the rate of infections (transitions $S \to C$) at time t. The second term $(\mathcal{A} \star K_C \star K_I \star K_R)(t)$ is the rate of individuals losing their immunity ($R \to S$) having undergone the full pathway of *S-C-I-R-S* transitions. In Eq. (1b) $\mathcal{A}(t)$ reappears as the entry rate to state C. The convolution $(\mathcal{A} \star K_C)(t)$ is the rate of delayed transition $C \to I$ of individuals that fall ill at time t. This rate reappears in Eq. (1d) as the entry rate into compartment I. Then $(\mathcal{A} \star K_C \star K_I)(t)$ is the rate of recovery $I \to R$ reoccurring in (1d) as the entry rate into compartment R. Finally, $(\mathcal{A} \star K_C \star K_I \star K_R)(t)$ in (1d) is the rate of individuals losing their immunity (transition $R \to S$) and reappears in (1a) as the entry rate into S. Let us consider for a moment (1b) more closely:

$$\frac{d}{dt}c(t) = \mathcal{A}(t) - \int_0^t K_C(t-\tau)\mathcal{A}(\tau) d\tau. \tag{4}$$

For our convenience we introduce the survival probability $\Phi_{C,I,R}(t)$ for individuals in compartments C, I, and R (also called persistence probability or survival function) (see, e.g., [14]),

$$\begin{aligned}\Phi_{C,I,R}(t) &= \text{Prob}(t_{C,I,R} > t) \\ &= \int_t^{\infty} K_{C,I,R}(\tau) d\tau = 1 - \int_0^t K_{C,I,R}(\tau) d\tau,\end{aligned} \tag{5}$$

indicating the probability that an individual which is entering compartments C, I, and R, respectively, at $t' = 0$ at time $t' = t$ still is (survives) in this compartment. Equation (5) captures all realizations with $t_{C,I,R} > t$ where $\frac{d}{dt}\Phi_{C,I,R}(t) = -K_{C,I,R}(t)$. We observe in this relation the initial condition $\Phi_{C,I,R}(0) = 1$ as a consequence of the normalization of the waiting-time PDFs and tells us that an individual is, with probability one, in a compartment at the instant when entering it. Further we have $\Phi_{C,I,R}(t \to \infty) \to 0+$, i.e., an individual survives only a finite time in compartments C, I, and R to enter eventually the susceptible state S. We hence can integrate (4) and rewrite it as

$$c(t) = \int_0^t \Phi_C(t-\tau)\mathcal{A}(\tau) d\tau = (\Phi_C \star \mathcal{A})(t), \tag{6}$$

where the initial condition $c(0) = 0$ is assumed. We can also verify this relation by its Laplace transform [Eq. (9b)] and directly by differentiating this expression with respect to t and using the initial condition $\Phi_C(0) = 1$. We interpret (6) as follows: $\mathcal{A}(\tau)d\tau$ is the fraction of walkers entering C during $[\tau, \tau + d\tau]$ and $\Phi_C(t-\tau)$ is the (survival) probability that this fraction still is in C after a delay of $t_C = t - \tau$, i.e., at time instant t where this expression sums up over the complete history of entries into C from 0 to time t. With these considerations, we can rewrite our *S-C-I-R-S* equations (1) in the equivalent integral forms

$$\begin{aligned}s(t) &= 1 - c(t) - j(t) - r(t), \\ c(t) &= (\Phi_C \star \mathcal{A})(t), \\ j(t) &= j_0 + (\mathcal{A} \star K_C \star \Phi_I)(t), \\ r(t) &= (\mathcal{A} \star K_C \star K_I \star \Phi_R)(t)\end{aligned} \tag{7}$$

for $t \geqslant 0$, where the initial conditions $s(0) = 1 - j_0$, $c(0) = 0$, $j(0) = j_0$, and $r(0) = 0$ are assumed.

B. Memoryless case: Exponentially distributed waiting times

It is worth considering exponential waiting-time kernels $K_{C,I,R}(t) = \xi_{C,I,R} e^{-t\xi_{C,I,R}}$ ($\xi_{C,I,R}^{-1} = \langle t_{C,I,R} \rangle$) where the survival functions are also exponentials $\Phi_{C,I,R}(t) = e^{-t\xi_{C,I,R}}$ and thus $K_{C,I,R}(t) = \xi_{C,I,R}\Phi_{C,I,R}(t)$. Substituting this into (1) and accounting for (7) takes us to the particular simple form without memory

$$\begin{aligned}
\frac{d}{dt}s(t) &= -\mathcal{A}(t) + \xi_R r(t),\\
\frac{d}{dt}c(t) &= \mathcal{A}(t) - \xi_C c(t),\\
\frac{d}{dt}j(t) &= \xi_C c(t) - \xi_I[j(t) - j_0],\\
\frac{d}{dt}r(t) &= \xi_I[j(t) - j_0] - \xi_R r(t)
\end{aligned} \tag{8}$$

for $t \geqslant 0$. Indeed, exponential densities stand out by the memoryless feature and the Markov property (see, e.g., [20–27] for details), thus the transition rates in (8) depend only on the instantaneous state $s(t)$, $c(t)$, $j(t)$, and $r(t)$ but not on the history of the evolution. Setting the transition rates on the left-hand side to zero yields straightforwardly the endemic state which we derive subsequently [Eqs. (21) and (22)] for arbitrary waiting-time kernels with existing means.

C. Arbitrary waiting-time distributions with memory

To explore the general cases with memory, consider now the equivalent representations (7) and (1) in the Laplace space

$$\hat{s}(\lambda) = \frac{1 - j_0}{\lambda} - \hat{\mathcal{A}}(\lambda)\frac{1 - \hat{K}_C(\lambda)\hat{K}_I(\lambda)\hat{K}_R(\lambda)}{\lambda}, \tag{9a}$$

$$\hat{c}(\lambda) = \hat{\mathcal{A}}(\lambda)\frac{1 - \hat{K}_C(\lambda)}{\lambda}, \tag{9b}$$

$$\hat{j}(\lambda) = \frac{j_0}{\lambda} + \hat{\mathcal{A}}(\lambda)\hat{K}_C(\lambda)\frac{1 - \hat{K}_I(\lambda)}{\lambda}, \tag{9c}$$

$$\hat{r}(\lambda) = \hat{\mathcal{A}}(\lambda)\hat{K}_C(\lambda)\hat{K}_I(\lambda)\frac{1 - \hat{K}_R(\lambda)}{\lambda}, \tag{9d}$$

where all Laplace transforms (LTs) depend on $\hat{\mathcal{A}}(\lambda)$ of the (unknown) infection rate and $\hat{\Phi}_{C,I,R}(\lambda) = \frac{1-\hat{K}_{C,I,R}(\lambda)}{\lambda}$ are the LTs of the survival probabilities. We further have that

$$\hat{s}(\lambda) + \hat{c}(\lambda) + \hat{j}(\lambda) + \hat{r}(\lambda) = \frac{1}{\lambda} = \int_0^\infty e^{-\lambda t} dt$$

as we deal with a constant population. We observe that in Eq. (9a) the term $\frac{1-\hat{K}_C(\lambda)\hat{K}_I(\lambda)\hat{K}_R(\lambda)}{\lambda}$ is the LT of the survival probability $\text{Prob}(t_C + t_R + t_I > t)$ [due to the PDF $(K_c \star K_I \star K_R)(t)$ of the random variable $t_C + t_I + t_R$], corresponding to individuals surviving in one of the compartments C, I, or R at time t. To shed more light on how the memory comes into play, we introduce a memory operator (for our convenience we employ here a slightly modified definition[2] as in [14,28])

$$\hat{\mathcal{M}}(\lambda) = \frac{\hat{K}(\lambda)}{\hat{\Phi}(\lambda)} = \lambda\frac{\hat{K}(\lambda)}{1 - \hat{K}(\lambda)} = \lambda\hat{\mathcal{L}}(\lambda). \tag{10}$$

[2]We suppress here subscripts C, I, and R.

Then reading $\hat{K}(\lambda) = \hat{\mathcal{M}}(\lambda)\hat{\Phi}(\lambda)$ as convolutions in the time domain, we can rewrite our *S-C-I-R-S* equations (1) (in the Caputo sense) of general (fractional) derivatives (see [15,16,29] and Appendix A) as

$$\begin{aligned}
\frac{d}{dt}s(t) &= -\mathcal{A}(t) + \int_0^t \mathcal{L}_R(t-\tau)\frac{d}{d\tau}r(\tau)d\tau,\\
\frac{d}{dt}c(t) &= \mathcal{A}(t) - \int_0^t \mathcal{L}_C(t-\tau)\frac{d}{d\tau}c(\tau)d\tau,\\
\frac{d}{dt}j(t) &= \int_0^t \mathcal{L}_C(t-\tau)\frac{d}{d\tau}c(\tau)d\tau\\
&\quad - \int_0^t \mathcal{L}_I(t-\tau)\frac{d}{d\tau}j(\tau)d\tau,\\
\frac{d}{dt}r(t) &= \int_0^t \mathcal{L}_I(t-\tau)\frac{d}{d\tau}j(\tau)d\tau\\
&\quad - \int_0^t \mathcal{L}_R(t-\tau)\frac{d}{d\tau}r(\tau)d\tau.
\end{aligned} \tag{11}$$

These equations show that the transition rates at time t have a complete memory of their previous values. Alternatively, we can write (11) in the Riemann-Liouville manner of general fractional derivatives (see Appendix A). For exponential waiting-time PDFs $K_{\text{exp}}(t) = \xi e^{-\xi t}$ we have $\hat{\mathcal{M}}_{\text{exp}}(\lambda) = \xi$; thus $\mathcal{M}_{\text{exp}}(t) = \xi\delta(t)$ (i.e., is null for $t > 0$ indicating lack of memory) and we easily recover above memoryless *S-C-I-R-S* equations (8).

D. Long waiting times: Time fractional case

The representation (11) is especially useful when we deal with fat-tailed waiting-time PDFs without existing means such as the Mittag-Leffler waiting-time PDF (MLPDF) (see [30] and references therein for explicit formulas). The MLPDF is a fractional generalization of the exponential PDF and has the LT [14,28] (and many others)

$$\tilde{K}_\beta(\lambda) = \frac{\xi}{\xi + \lambda^\beta}, \quad \beta \in (0, 1),\ \xi > 0, \tag{12}$$

where, due to the fat tail, the mean waiting time $-\frac{d}{d\lambda}\tilde{K}_\beta(\lambda)|_{\lambda=0} \to \infty$ does not exist as $\beta \in (0, 1)$ (occurrence of extremely long waiting times). For $\beta = 1$ Eq. (12) retrieves the LT of the exponential density. Expanding the LT for λ small $\tilde{K}_\beta(\lambda) \sim 1 - \frac{\lambda^\beta}{\xi}$, Laplace inversion shows that MLPDF has a fat power-law tail $K_\beta(t) \sim \frac{\beta}{\Gamma(1-\beta)}\frac{t^{-\beta-1}}{\xi}$ $(t \to \infty)$ corresponding to a long memory. For the Mittag-Leffler case we have for (10)

$$\hat{\mathcal{L}}_\beta(\lambda) = \xi\lambda^{-\beta}, \tag{13}$$

where $\lambda^{-\beta}$ corresponds to the Riemann-Liouville fractional integral of degree β and $\hat{\mathcal{M}}_\beta(\lambda) = \xi\lambda^{1-\beta}$ the Riemann-Liouville (RL) fractional derivative of order $1 - \beta$. Denoting by D_t^ν the RL fractional derivative, it is sufficient to consider the range $\mu \in (0, 1)$ defined by [30]

$$D_t^\mu f(t) = \frac{d}{dt}\int_0^t \frac{(t-\tau)^{-\mu}}{\Gamma(1-\mu)}f(\tau)d\tau, \quad \mu \in (0, 1) \tag{14}$$

having LT $\lambda^\mu \hat{f}(\lambda)$ and with the definition of the Caputo fractional derivative

$$\frac{d^\mu}{dt^\mu} f(t) = \int_0^t \frac{(t-\tau)^{-\mu}}{\Gamma(1-\mu)} \frac{d}{d\tau} f(\tau) d\tau = D_t^\mu f(t) - f(0)\frac{t^{-\mu}}{\Gamma(1-\mu)}, \quad \mu \in (0,1) \tag{15}$$

with LT $\lambda^\mu \hat{f}(\lambda) - f(0)\lambda^{\mu-1}$. Consult Appendix A and [29] for the connections with general (fractional) derivatives. In the limit $\mu \to 1-$ both Caputo and RL fractional derivatives converge to the first-order standard derivative where $\frac{t^{-\mu}}{\Gamma(1-\mu)} \to \delta(t)$. Using the feature

$$\frac{d^\mu}{dt^\mu}[f(t) - f(0)] = \frac{d^\mu}{dt^\mu} f(t) = D_t^\mu [f(t) - f(0)], \tag{16}$$

we can then write (11) when all waiting times $t_{C,I,R}$ are drawn from MLPDFs in terms of Caputo fractional derivatives as

$$\begin{aligned}
\frac{d}{dt} s(t) &= -\mathcal{A}(t) + \xi_R \frac{d^{1-\beta}}{dt^{1-\beta}} r(t), \\
\frac{d}{dt} c(t) &= \mathcal{A}(t) - \xi_C \frac{d^{1-\beta}}{dt^{1-\beta}} c(t), \\
\frac{d}{dt} j(t) &= \xi_C \frac{d^{1-\beta}}{dt^{1-\beta}} c(t) - \xi_I \frac{d^{1-\beta}}{dt^{1-\beta}} j(t), \\
\frac{d}{dt} r(t) &= \xi_I \frac{d^{1-\beta}}{dt^{1-\beta}} j(t) - \xi_R \frac{d^{1-\beta}}{dt^{1-\beta}} r(t),
\end{aligned} \tag{17}$$

retrieving for $\beta = 1$ the equations (8) of exponential waiting-time PDFs [see (15) and (16)]. Indeed, the time-fractional case with fat-tailed waiting-time distributions is of utmost importance, deserving further thorough investigation (see Appendix B for a brief account).

E. Endemic equilibrium for waiting-time PDFs with existing mean

Here we confine ourselves to waiting-time PDFs with existing means. The endemic state is defined as the long-time limit of the evolution. That is, we seek a stationary (constant solution) $[s(t), c(t), j(t), r(t)] \to [S_e, C_e, J_e, R_e]$ and $\mathcal{A}(t) \to A_e = \beta J_e S_e$, which also is the asymptotic solution for $t \to \infty$ if the endemic state is stable. This solution can be obtained from Eqs. (9) in the limit of small λ, where these equations then take [with $\hat{s}(\lambda) \to S_e/\lambda$, etc.] the form

$$\begin{aligned}
S_e &= 1 - j_0 - \lim_{\lambda\to 0} \hat{\mathcal{A}}(\lambda)[1 - K_C(\lambda)K_I(\lambda)\hat{K}_R(\lambda)], \\
C_e &= \lim_{\lambda\to 0} \hat{\mathcal{A}}(\lambda)[1 - \hat{K}_C(\lambda)], \\
J_e &= j_0 + \lim_{\lambda\to 0} \hat{\mathcal{A}}(\lambda)\hat{K}_C(\lambda)[1 - \hat{K}_I(\lambda)], \\
R_e &= \lim_{\lambda\to 0} \hat{\mathcal{A}}(\lambda)\hat{K}_C(\lambda)\hat{K}_I(\lambda)[1 - \hat{K}_R(\lambda)],
\end{aligned} \tag{18}$$

with

$$\hat{\mathcal{A}}(\lambda) \approx \frac{A_e}{\lambda} + A_0 + A_1\lambda + \cdots,$$

which has to be considered for $\lambda \to 0$ where the lowest order in λ determines the endemic equilibrium. Now with

$$\hat{K}(\lambda) = \int_0^\infty e^{-\lambda\tau} K(\tau) d\tau \approx \int_0^\infty (1 - \lambda\tau) K(\tau) d\tau + o(\lambda) = 1 - \lambda\langle\tau\rangle + o(\lambda), \tag{19}$$

where the angular brackets denote mean values and $o(\lambda)$ stands for the Landau symbol. Thus we have

$$\hat{K}_{C,I,R}(\lambda) = 1 - \lambda\langle t_{C,I,R}\rangle + o(\lambda) \tag{20}$$

and $\hat{K}_C(\lambda)\hat{K}_I(\lambda)\hat{K}_R(\lambda) = 1 - \lambda\langle t_C + t_I + t_R\rangle + o(\lambda) = 1 - \lambda\langle T\rangle + o(\lambda)$ and as stated previously we assume that the means exist. Therefore,

$$\lim_{\lambda\to 0} \hat{\Phi}_{C,I,R}(\lambda) = \lim_{\lambda\to 0} \frac{1 - \hat{K}_{C,I,R}(\lambda)}{\lambda} = -\frac{d}{d\lambda}\hat{K}_{C,I,R}(\lambda)\Big|_{\lambda=0} = \langle t_{C,I,R}\rangle.$$

Then we get straightforwardly, for the lowest orders in λ, the endemic equilibrium of

$$\begin{aligned}
S_e &= 1 - j_0 - A_e\langle T\rangle, \\
C_e &= A_e\langle t_C\rangle, \\
J_e &= j_0 + A_e\langle t_I\rangle, \\
R_e &= A_e\langle t_R\rangle,
\end{aligned} \tag{21}$$

and with our assumption $A_e = \beta J_e S_e$ we arrive at

$$\begin{aligned}
S_e(J_e) &= \frac{1 - j_0}{1 + \beta\langle T\rangle J_e}, \\
C_e(J_e) &= \frac{(1 - j_0)\beta\langle t_C\rangle J_e}{1 + \beta\langle T\rangle J_e}, \\
J_e &= j_0 + \beta\langle t_I\rangle J_e \frac{1 - j_0}{1 + \beta\langle T\rangle J_e}, \\
R_e(J_e) &= \frac{(1 - j_0)\beta\langle t_R\rangle J_e}{1 + \beta\langle T\rangle J_e}.
\end{aligned} \tag{22}$$

Consider now the third relation in (22), which is an implicit equation for J_e leading to

$$J_e^2 - 2aJ_e - b = 0, \tag{23}$$

where we have introduced

$$\begin{aligned}
a &= \frac{j_0}{2} + \frac{\beta\langle t_I\rangle(1 - j_0) - 1}{2\beta\langle T\rangle} \\
&= \frac{\langle t_R + t_C\rangle j_0}{2\langle T\rangle} + \frac{R_0 - 1}{2\beta\langle T\rangle}, \quad R_0 = \beta\langle t_I\rangle \\
b &= \frac{j_0}{\beta\langle T\rangle}.
\end{aligned} \tag{24}$$

The quantity $R_0 = \beta\langle t_I\rangle$ can be interpreted as the basic reproduction number and is a crucial (control) parameter; we will return to this interpretation subsequently. Equation (23) has the roots

$$(J_e)_{1,2} = a \pm \sqrt{a^2 + b}. \tag{25}$$

Clearly the endemic equilibrium exists only for those roots with $J_e \in [0, 1]$, with the full endemic state then determined by (22). For $b = 0$ ($j_0 = 0$) one root is zero, corresponding to the healthy state $S_e = 1$. The second root is $J_e(j_0 = 0) = 2a = \frac{R_0-1}{\beta\langle T\rangle} \in [0, 1)$ for $R_0 = \beta\langle t_I\rangle > 1$, which therefore is the condition of the existence of an endemic state for $j_0 = 0$. In Appendix B we show for waiting-time PDFs with existing means that $R_0 > 1$ also is the condition that the healthy state is unstable and thus an epidemic can start to spread. We also show there that the healthy state is always unstable if $K_I(t)$ has a fat tail (i.e., infinite mean). Indeed, for $\langle t_I\rangle \to \infty$ (β, $\langle t_C\rangle$, and $\langle t_R\rangle$ kept finite) we have $R_0 \to \infty$ and thus $J_e(j_0 = 0) \sim \langle t_I\rangle/\langle T\rangle \to 1$ and for $\beta \to \infty$ ($\langle t_I\rangle$, $\langle t_C\rangle$, and $\langle t_R\rangle$ finite) we get $J_e(j_0 = 0) \to \langle t_I\rangle/\langle T\rangle$.

Consider now $j_0 > 0$ and $R_0 > 1$. Then we have $a < 1$ as $\frac{\langle t_R+t_C\rangle j_0}{2T} < \frac{1}{2}$, $\frac{R_0-1}{2\beta\langle T\rangle} < \frac{1}{2}$, and $b < 1$ and thus the only positive root is

$$(J_e)_1 = a + \sqrt{a^2 + b}, \tag{26}$$

whereas the other $(J_e)_2 = a - \sqrt{a^2 + b} < 0$. The endemic state exists if $(J_e)_1 \leqslant 1$. As a and b are monotonically increasing functions of j_0 let us check the root for the maximum value $j_0 = 1$ where $a(j_0 = 1) = \frac{1}{2} - \frac{1}{2\beta T} = \frac{1}{2}(1 - \epsilon)$ and $b(j_0 = 1) = \frac{1}{\beta\langle T\rangle} = \epsilon$. Then we get

$$\begin{aligned} J_e(j_0)|_{j_0=1} &= \frac{1}{2}[1 - \epsilon + \sqrt{(1-\epsilon)^2 + 4\epsilon}] \\ &= \frac{1 - \epsilon + \sqrt{(1+\epsilon)^2}}{2} = 1, \end{aligned} \tag{27}$$

i.e., the initial and endemic states coincide $j_0 = J_e(1) = 1$, where we infer that $j = 1$ (for $R_0 > 1$) should be a stable endemic state. From the monotonicity of $J_e(j_0)$ [see (24)] we can see that

$$\frac{R_0 - 1}{\beta\langle T\rangle} \leqslant J_e(j_0) \leqslant J_e(j_0)|_{j_0=1} = 1,$$

i.e., in the entire range $j_0 \in [0, 1]$ the endemic value is given by the positive root (26) together with (24). This behavior is shown in Fig. 1, where we draw J_e versus j_0 for different values of $R_0 > 1$. One can see that J_e is monotonically increasing with R_0 when $\langle t_R\rangle$, $\langle t_C\rangle$, and j_0 are kept constant.

We focus now on initial conditions $s_0 = 1^-$ and $j_0 = 0^+$ (healthy state). The endemic equilibrium (22) then is written

$$\begin{aligned} S_e &= \frac{1}{R_0}, \\ C_e &= \frac{R_0 - 1}{R_0}\frac{\langle t_C\rangle}{\langle T\rangle}, \\ J_e &= \frac{R_0 - 1}{R_0}\frac{\langle t_I\rangle}{\langle T\rangle}, \\ R_e &= \frac{R_0 - 1}{R_0}\frac{\langle t_R\rangle}{\langle T\rangle}, \end{aligned} \tag{28}$$

for $\langle T\rangle = \langle t_C + t_I + t_R\rangle$ and $R_0 = \beta\langle t_I\rangle$, and exists solely for $R_0 > 1$, depending only on R_0 and the mean waiting times $\langle t_{C,I,R}\rangle$. We may consider the following limiting cases.

Case 1. Here $\langle t_R\rangle \to \infty$ (infinitely long immunity) and $\langle t_C\rangle$, $\langle t_I\rangle$, and β are kept constant.

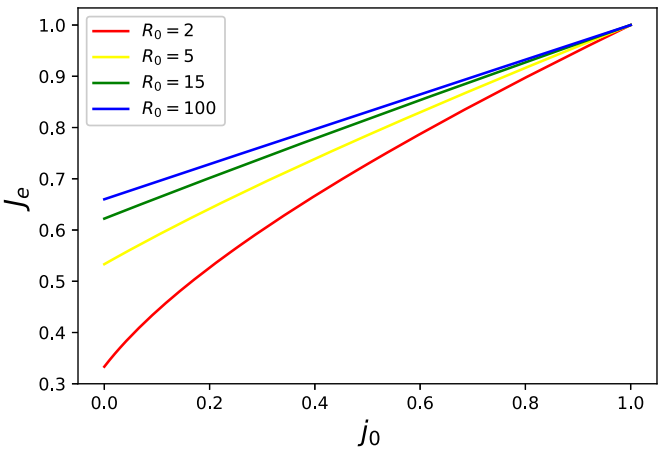

FIG. 1. Endemic value $J_e(j_0, R_0)$ vs j_0 from Eq. (26) with (24) for different values of $R_0 > 1$; for all curves we have set $\langle t_C\rangle = \langle t_R\rangle = 5$ and $\langle t_I\rangle = 20$.

Then we have $\frac{\langle t_R\rangle}{\langle T\rangle} \to 1$ and $\frac{\langle t_C\rangle}{\langle T\rangle}$, $\frac{\langle t_I\rangle}{\langle T\rangle} \to 0$ and hence $S_e = \frac{1}{R_0}$ remains unchanged; thus $C_e, J_e \to 0$ and $R_e \to \frac{R_0-1}{R_0}$ with $S_e + R_e = 1$, which corresponds to a fully healthy population (susceptible or immune) with $C_e + J_e \to 0$, i.e., the disease in the long-time limit dies out.

Case 2. In the same way, the limits $\langle t_I\rangle \to \infty$ (long illness time) and long incubation time $\langle t_C\rangle \to \infty$ are straightforward, where the endemic values of respective compartments with infinite waiting times tend to $\frac{R_0-1}{R_0}$ with unchanged $S_e = \frac{1}{R_0}$. This corresponds to the fact that the individuals remain eventually trapped in the respective compartments (C or I) with infinite waiting times and thus the cyclic transition pathway $S \to \cdots \to S$ is suppressed. We infer that in the limiting cases 1 and 2 the endemic states are stable, similar to the class of classical SIR models, and do not exhibit oscillatory instabilities.

III. δ-DISTRIBUTED WAITING TIMES

An instructive case consists in the deterministic limit when the sojourn times in the compartments for all walkers are constant. Then the waiting-time PDFs are Dirac δ functions

$$K_{C,I,R}(t) = \delta(t - t_{C,I,R}) \tag{29}$$

with LTs $\hat{K}_{C,I,R}(\lambda) = e^{-\lambda t_{C,I,R}}$. Recall now the convolution of two δ kernels

$$\delta(t - t_1) \star \delta(t - t_2) = \delta(t - t_1 - t_2),$$

which yields a new δ kernel with a shifted peak at $t_1 + t_2$. With this observation we have $(K_C \star K_I)(t) = \delta(t - t_C - t_I)$ and $(K_C \star K_I \star K_R)(t) = \delta(t - t_C - t_I - t_R)$. Then the *S-C-I-R-S* equations (1) read

$$\begin{aligned} \frac{d}{dt}s(t) &= -\mathcal{A}(t) + \mathcal{A}(t - t_C - t_I - t_R), \\ \frac{d}{dt}c(t) &= \mathcal{A}(t) - \mathcal{A}(t - t_C), \end{aligned}$$

$$\frac{d}{dt}j(t) = \mathcal{A}(t - t_C) - \mathcal{A}(t - t_C - t_I),$$
$$\frac{d}{dt}r(t) = \mathcal{A}(t - t_C - t_I) - \mathcal{A}(t - t_C - t_I - t_R). \quad (30)$$

Note that $\mathcal{A}(t) = \mathcal{A}(j(t), s(t))$ is causal, i.e., all functions with negative time arguments are vanishing. For $t < t_C$ the infected individuals accumulate in the compartment C and for $t \geqslant t_C$ some start to leave compartment C to enter I with the delayed rate $A(t - t_C)$. Then for $t \geqslant t_C + t_I$ the first individuals are healed, starting transitions $I \to R$ with rate $A(t - t_C - t_I)$. Finally, for $t \geqslant t_C + t_I + t_R$ transitions $R \to S$ occur due to individuals losing their immunity. From these observations we can infer that

$$c(t) = \int_0^t \mathcal{A}(\tau)d\tau - \Theta(t - t_C)\int_0^{t-t_C} \mathcal{A}(\tau)d\tau,$$
$$j(t) = j_0 + \Theta(t - t_C)\int_0^{t-t_C} \mathcal{A}(\tau)d\tau - \Theta(t - t_C - t_I) \times \int_0^{t-t_C-t_I} \mathcal{A}(\tau)d\tau,$$
$$r(t) = \Theta(t - t_C - t_I)\int_0^{t-t_C-t_I} \mathcal{A}(\tau)d\tau - \Theta(t - t_C - t_I - t_R) \times \int_0^{t-t_C-t_I-t_R} \mathcal{A}(\tau)d\tau, \quad (31)$$

where $\Theta(\tau)$ denotes the Heaviside unit step function defined as $\Theta(\tau) = 1$ for $\tau \geqslant 0$ and $\Theta(\tau) = 0$ for $\tau < 0$. We can see for sharp waiting times the Heaviside functions switch on and off the respective transitions between compartments. It is worth mentioning that (31) is consistent with (7) when we take into account the survival probabilities

$$\Phi_{C,I,R}(t) = \int_t^\infty \delta(\tau - t_{C,I,R})d\tau = \Theta(t_{C,I,R} - t) = 1 - \Theta(t - t_{C,I,R}), \quad (32)$$

i.e., $\Phi_{C,I,R}(t) = 1$ for $t < t_{C,I,R}$ (survival in C, I, and R, respectively) and $\Phi_{C,I,R}(t) = 0$ for $t > t_{C,I,R}$ (death, having left C, I, and R, respectively). From Eqs. (31) we find the endemic equilibrium of S_e, C_e, J_e, and R_e representing a stationary solution of (30). Plugging the stationary value $\mathcal{A}_e = \beta J_e S_e$ into (31), we rearrive at Eqs. (22) with $t_{C,I,R} = \langle t_{C,I,R}\rangle$ for Dirac δ distributions.

Stability analysis of endemic and healthy states

Here we investigate the stability of the endemic equilibrium for healthy initial conditions $s_0 = 1$ ($j_0 = 0$) for δ-distributed waiting times. To this end we set

$$s(t) = S_e + ue^{\mu t},$$
$$c(t) = C_e + ve^{\mu t},$$
$$j(t) = J_e + we^{\mu t},$$
$$r(t) = R_e + xe^{\mu t}, \quad (33)$$

where u, v, w, and x are small time-independent constants. Clearly, at least one of these equations is redundant as $s + c + j + r = 1$. Then it follows that $\mathcal{A}(t) \approx A_e + A_0(u, w)e^{\mu t}$, where we take into account only the linear orders in u, v, w, and x. Therefore, $A_e = \beta J_e S_e$ and $A_0(u, w) = \beta(uJ_e + wS_e)$. Plugging this into (30) leads to the system of equations

$$A_0(u, w)(1 - e^{-\mu T}) + \mu u = 0,$$
$$A_0(u, w)(1 - e^{-\mu t_C}) - \mu v = 0,$$
$$A_0(u, w)e^{-\mu t_C}(1 - e^{-\mu t_I}) - \mu w = 0,$$
$$A_0(u, w)e^{-\mu(t_C+t_I)}(1 - e^{-\mu t_R}) - x\mu = 0. \quad (34)$$

We can eliminate $v = A_0(u, w)\frac{1-e^{-\mu t_C}}{\mu}$ and $x = A_0(u, w)e^{-\mu(t_C+t_I)}\frac{1-e^{-\mu t_R}}{\mu}$, which are uniquely determined by u and w. Therefore, the solvability condition is determined uniquely by the first and third equation for s and j containing only the coefficients u and w. The complete determinant of the system (34) leads to

$$\begin{vmatrix} \beta J_e(1 - e^{-\mu T}) + \mu & \beta S_e(1 - e^{-\mu T}) \\ \beta J_e e^{-\mu t_C}(1 - e^{-\mu t_I}) & \beta S_e e^{-\mu t_C}(1 - e^{-\mu t_I}) - \mu \end{vmatrix} \mu^2 = 0. \quad (35)$$

We have $\mu = 0$ as a threefold eigenvalue and with one nonzero eigenvalue μ_1 determined by

$$\mu = \beta S_e e^{-\mu t_C}(1 - e^{-\mu t_I}) - \beta J_e(1 - e^{-\mu T}) \quad (36)$$

and hence $\mu_1 = \mu_1(\beta, j_0, t_C, t_I, t_R)$. However, we will see that we can reduce the set of pertinent parameters. For the outbreak of an epidemic, it is necessary that the healthy (initial) state $s_0 = 1$ becomes unstable. To explore this issue we consider $s(t) = s_0 + ue^{\mu t}$ and $j(t) = j_0 + we^{\mu t}$ with $s_0 = 1$ and $j_0 = 0$. Then we get the solvability condition by replacing in (35) $J_e \to j_0 = 0$ and $S_e \to s_0 = 1$ in the form

$$\tilde{\mu} = R_0 e^{-\tilde{\mu}t_1}[1 - e^{-\tilde{\mu}}) = g(\tilde{\mu}, R_0), \quad (37)$$

where we introduce

$$\tilde{\mu} = t_I\mu, \quad t_1 = \frac{t_C}{t_I}, \quad t_2 = \frac{T}{t_I} = 1 + t_1 + \frac{t_R}{t_I}. \quad (38)$$

The healthy state becomes unstable if there is a positive solution $\tilde{\mu}_0 > 0$ of this equation. Clearly there is a positive root only if $\frac{d}{d\tilde{\mu}}g(\tilde{\mu}, R_0)|_{\tilde{\mu}=0} = R_0 > 1$; otherwise the healthy state is stable. This justifies our interpretation of R_0 as the basic reproduction number where the healthy state is unstable for $R_0 > 1$ and thus the epidemic starts to spread.

It is instructive to connect this interpretation with the common definition of R_0. The (dimensionless) basic reproduction number R_0 is defined as the expected number of infections caused by one infectious individual in a healthy (susceptible) population. We get this information when we multiply Eq. (1b) with the total number of individuals Z, where $Z\mathcal{A}(t)$ then indicates the number of new infections per time unit. Considering this quantity at $t = 0$ for the initial condition $j_0 = \frac{1}{Z}$ and $s_0 = 1 - j_0$ [initial condition of one infected individual $Z_I(0) = j_0 Z = 1$ in a healthy, i.e., susceptible, population $Z_S(0) = s_0 Z = Z - 1$] takes us to

$$\left.\frac{dZ_c(t)}{dt}\right|_{t=0} = Z\beta s(t)j(t)|_{t=0} = \left.\frac{\beta}{Z}Z_S(t)Z_I(t)\right|_{t=0} = \beta\frac{Z-1}{Z} \to \beta, \quad Z \gg 1,$$

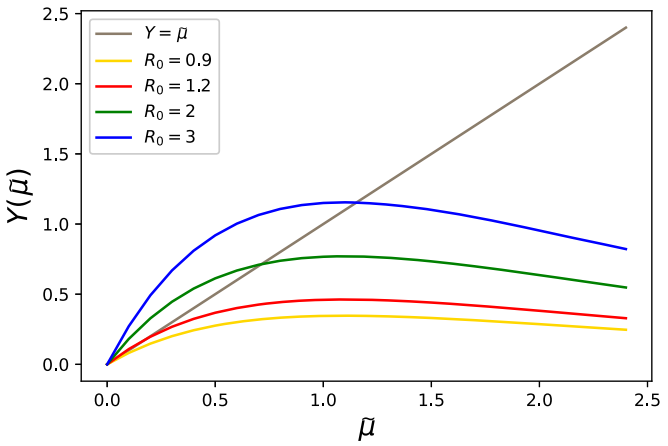

FIG. 2. Plot of $g(\tilde{\mu}, R_0) = R_0 e^{-\tilde{\mu}t_1}(1 - e^{-\tilde{\mu}})$ for different values of R_0. For $R_0 = 0.9$ (lower curve) the healthy state is stable. For the other curves $R_0 > 1$ the healthy state is unstable. In all plots $t_1 = t_C/t_I = 0.5$.

which is the number of new infections per time unit at $t = 0$. Assuming this rate is constant during the average period of infection $\langle t_I \rangle$ (given this mean exists) yields the average number of new infections caused by the first infected walker during the period t_I of his infection (in a susceptible population) as $R_0 = \beta \langle t_I \rangle$. This is indeed the exact result of our model as we show in Appendix B. We demonstrate there that the condition for an outbreak (condition of instability of the healthy initial state) is $R_0 = \beta \langle t_I \rangle > 1$. This can also be seen more closely on the right-hand side of (37), where $g(\tilde{\mu}, R_0)$ is a concave function of $\tilde{\mu}$ (see Fig. 2). We have for $\tilde{\mu}$ small the expansion $g(\tilde{\mu}, R_0) = R_0\tilde{\mu} + O(\tilde{\mu}^2) > \tilde{\mu}$ only if $R_0 > 1$ and always $g(\tilde{\mu}, R_0) \to 0 < \tilde{\mu}$ as $\mu \to \infty$. Therefore, a positive root $\mu_0(R_0) > 0$ exists only for $R_0 > 1$. This behavior is shown in Fig. 2, where $\mu_0(R_0)$ increases monotonically with R_0 enhancing the (nonpersistent) exponential growth of $j(t)$ at the outbreak of the epidemic.

Returning to the stability analysis of the endemic state, we rescale (36) with (38) as

$$\tilde{\mu} = R_0 S_e e^{-\tilde{\mu}t_1}(1 - e^{-\tilde{\mu}}) - R_0 J_e(1 - e^{-\tilde{\mu}t_2}). \tag{39}$$

At the threshold of an oscillatory instability, the eigenvalue is purely imaginary. Plugging $\tilde{\mu} = i\omega$ into (39) and separating real and imaginary parts yields the two conditions

$$\begin{aligned} f_1(r_0, \omega) &= \cos \omega t_1 - \cos \omega(t_1 + 1) - r_0(1 - \cos \omega t_2) = 0, \\ f_2(r_0, \omega) &= \omega + \sin \omega t_1 - \sin \omega(t_1 + 1) + r_0 \sin \omega t_2 = 0, \end{aligned} \tag{40}$$

which need to be simultaneously fulfilled for an oscillatory (Hopf) instability where we introduced the reduced control parameter $r_0 = J_e R_0 = (R_0 - 1)/t_2$.

On the left-hand side of Fig. 3 we plot the zero lines of f_i in the (r_0, ω) plane for $t_1 = \frac{1}{2}$ and $t_2 = 10$. They intersect at $r_0 \approx 0.063$ and $\omega = 0.35$, corresponding to a critical $R_0 \approx 1.63$. The right-hand side of Fig. 3 shows numerical solutions of the full delay system (30) with the same parameters t_1 and t_2. The system is solved using an Euler forward scheme with fixed time step $\delta t = 10^{-4}$. The initial conditions are $j_0 = 10^{-4}$, $s_0 = 1 - j_0$, and $r_0 = c_0 = 0$ close to the healthy state. We varied R_0 from 1.5 (subcritical, top left) to 2.0 (bottom right frame). Clearly for $R_0 = 1.7$ the stable focus turns into a limit cycle that becomes wider with increasing R_0.

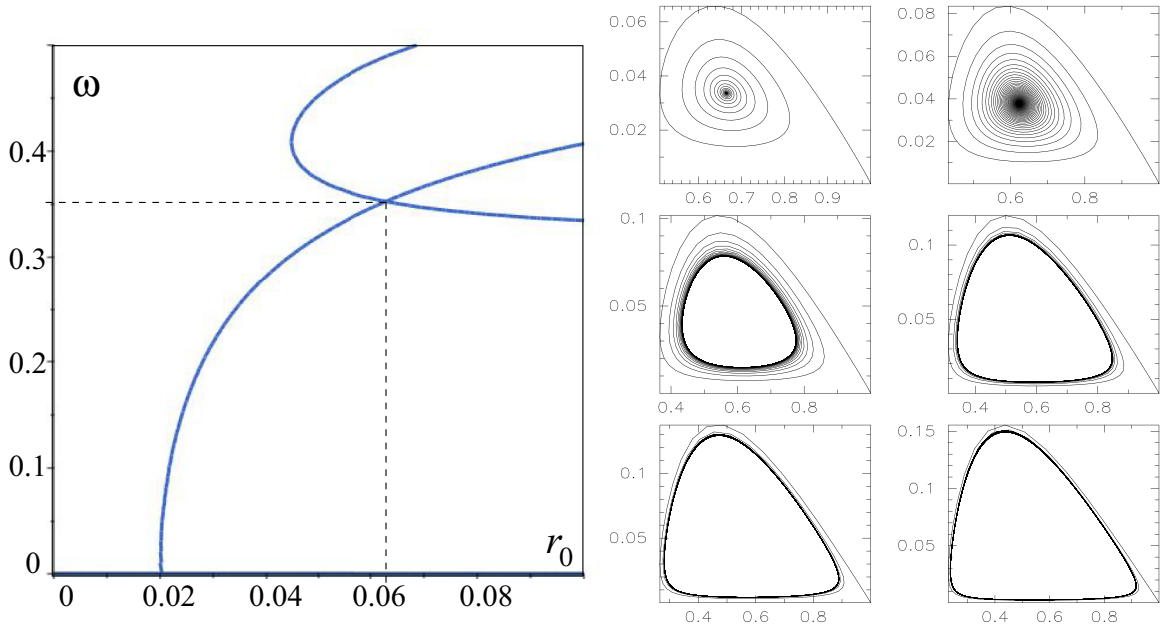

FIG. 3. Shown on the left is the intersection of the contour lines of f_1, $f_2 = 0$ of (40) which yields $(\omega, r_0) \approx (0.35, 0.063)$. Shown on the right are numerical solutions of the fully nonlinear delay system (30) for $R_0 = 1.5$ (top left) to $R_0 = 2.0$ in the (j, s) plane. A limit cycle is born at $R_0 \approx 1.63$.

IV. MICROSCOPIC MODEL AND COMPUTER SIMULATIONS

A. Simple random-walk model

To explore the *S-C-I-R-S* phenomenology, we combine this model with a multiple-random-walker approach which we implemented in a PYTHON code [31]. In this random walk Z walkers navigate independently on a periodic two-dimensional lattice. Each walker performs at integer times $t = 0, 1, 2, \ldots$ instantaneous independent random steps to a nearest-neighbor lattice point (simple walk). The position of walker j ($j = 1, \ldots, Z$) can be described by the random variables

$$\begin{aligned} x_j(t) &= x_j(t-1) + \eta_x^{(j)}(t), \\ y_j(t) &= y_j(t-1) + \eta_y^{(j)}(t) \end{aligned} \tag{41}$$

for $t = 1, 2, \ldots$, with the random steps $(\eta_x^{(j)}(t), \eta_y^{(j)}(t)) = (1, 0), (-1, 0), (0, 1), (0, -1)$ occurring with probability $\frac{1}{4}$. This simple multiwalker motion is a microscopic model with scaling limits to (standard) Brownian motion [32]. We assume an $N_x = N_y = N$ periodic lattice with $x^{(j)}(t) = x^{(j)}(t) \mathrm{mod} N$ and $y^{(j)}(t) = y^{(j)}(t) \mathrm{mod} N$ for the position of each walker j. In order to connect the random walk with the epidemic dynamics we apply the following infection rule [11]: If a walker $j \in I$ meets a walker $k \in S$ on the same lattice point (collision of an infected-infectious and a susceptible walker), i.e.,

$$\begin{aligned} & j \in I \wedge k \in S \\ & \wedge x_j(t) = x_k(t) \\ & \wedge y_j(t) = y_k(t), \end{aligned} \tag{42}$$

then the susceptible walker k gets infected with probability P_{inf} and undergoes an instantaneous transition $S \to C$ followed by the transition pathway as described previously. The infection probability P_{inf} is constant for all walkers and time independent. The random paths of the walkers are not affected by transitions between the compartments or collisions of walkers. In the simulations at each integer time instant t, we count the populations $Z_{S,C,I,R}(t)$ in the compartments where the total population $Z = Z_S(t) + Z_C(t) + Z_I(t) + Z_R(t)$ remains constant over time. As in the macroscopic model, we focus on the fractions $s(t) = Z_S(t)/Z$, $c(t) = Z_C(t)/Z$, $j(t) = Z_I(t)/Z$, and $r(t) = Z_R(t)/Z$.

We implement the mutually independent waiting times $t_{C,I,R}$ as random numbers drawn from specific Γ PDFs $K_{C,I,R}(t)$. The Γ distribution provides sufficient flexibility to generate a wide range of possible behaviors such as sharp δ peaks, broadly scattered waiting times with a maximum, or a monotonically decreasing PDF. The Γ (also called Erlang) PDF is written

$$K_{\xi,\alpha}(\tau) = \frac{\xi^\alpha \tau^{\alpha-1}}{\Gamma(\alpha)} e^{-\xi\tau}, \quad \alpha, \xi > 0, \tag{43}$$

where α is the so-called shape parameter and $1/\xi$ the timescale parameter. The Γ PDF has a maximum for $\alpha > 1$ at $t_m = \frac{\alpha-1}{\xi}$ and is monotonically decreasing for $\alpha \leqslant 1$ and weakly singular at $t = 0$ for $\alpha < 1$. For $\alpha = 1$ we get the exponential PDF $K_{\xi,1}(\tau) = \xi e^{-\xi\tau}$. Some cases of Γ PDFs are drawn in histograms of Fig. 4. Useful is its Laplace transform

$$\hat{K}_{\xi,\alpha}(\lambda) = \int_0^\infty e^{-\lambda\tau} K_{\xi,\alpha}(\tau) d\tau = \frac{\xi^\alpha}{(\lambda+\xi)^\alpha}, \tag{44}$$

from which we can easily retrieve $\hat{K}_{\xi,\alpha}(\lambda)|_{\lambda=0} = 1$ (normalization), $\langle t \rangle = -\frac{d}{d\lambda}\hat{K}_{\xi,\alpha}(\lambda)|_{\lambda=0} = \frac{\alpha}{\xi}$ (mean waiting time), and $\mathcal{V} = \langle t^2 \rangle - \langle t \rangle^2 = \frac{\alpha}{\xi^2}$ (variance). In the simulations, to generate constant (sharp) waiting times, we use the feature (see, e.g., [11])

$$\lim_{\xi\to\infty} K_{\xi,\alpha=\xi\tau_0}(\tau) = \delta(\tau - \tau_0), \tag{45}$$

where the mean $\tau_0 = \langle \tau \rangle$ is kept constant in this limit and the variance is vanishing. This limit is easily seen in the Laplace space

$$\begin{aligned} \lim_{\xi\to\infty} \hat{K}_{\xi,\xi\tau_0}(\lambda) &= \lim_{\xi\to\infty} \left(1 + \frac{\lambda}{\xi}\right)^{-\xi\tau_0} \\ &= e^{-\tau_0\lambda} = \int_0^\infty e^{-\lambda t} \delta(t - \tau_0) dt. \end{aligned} \tag{46}$$

B. Validation of the macroscopic *S-C-I-R-S* model and case study

In the simulations we remove unimportant fluctuations by recording the ensemble-averaged[3] compartment populations $\langle s(t) \rangle$, $\langle c(t) \rangle$, $\langle r(t) \rangle$, and $\langle j(t) \rangle$. We average numerically over a number of equivalent random-walk realizations with identical parameters, waiting-time distributions, and observation times. Each realization employs different random numbers (PYTHON seeds) for the waiting times and random walk. We perform a case study to validate the macroscopic equations (28) for the endemic equilibrium which exists for $R_0 = \beta \langle t_I \rangle > 1$. We realize natural initial conditions close to the healthy state with one infected walker (in compartment I) and $Z - 1$ susceptible walkers at $t = 0$ (start of the experiment). In all computer experiments the walkers have random initial positions on the lattice. We determine the endemic equilibrium values numerically by using the asymptotic relation

$$[S_e, C_e, J_e, R_e]_{\mathrm{num}}(t) \approx \frac{1}{t} \sum_{r=1}^{t} \langle [s(r), c(t), j(t), r(t)] \rangle \tag{47}$$

converging for $t \to \infty$ to the endemic state S_e, C_e, J_e, or R_e if it exists. We measure the accordance of our macroscopic endemic equations (28) with the random-walk approach by computing the ratios of the numerically determined endemic values and the values computed with (28),

$$\begin{aligned} r_C &= \frac{(C_e)_{\mathrm{num}}}{[1 - (S_e)_{\mathrm{num}}]\langle t_C \rangle / \langle T \rangle}, \\ r_I &= \frac{(J_e)_{\mathrm{num}}}{[1 - (S_e)_{\mathrm{num}}]\langle t_I \rangle / \langle T \rangle}, \\ r_R &= \frac{(R_e)_{\mathrm{num}}}{[1 - (S_e)_{\mathrm{num}}]\langle t_R \rangle / \langle T \rangle}, \end{aligned} \tag{48}$$

[3]We denote here ensemble averages of random functions $B(t)$ by $\langle B(t) \rangle$.

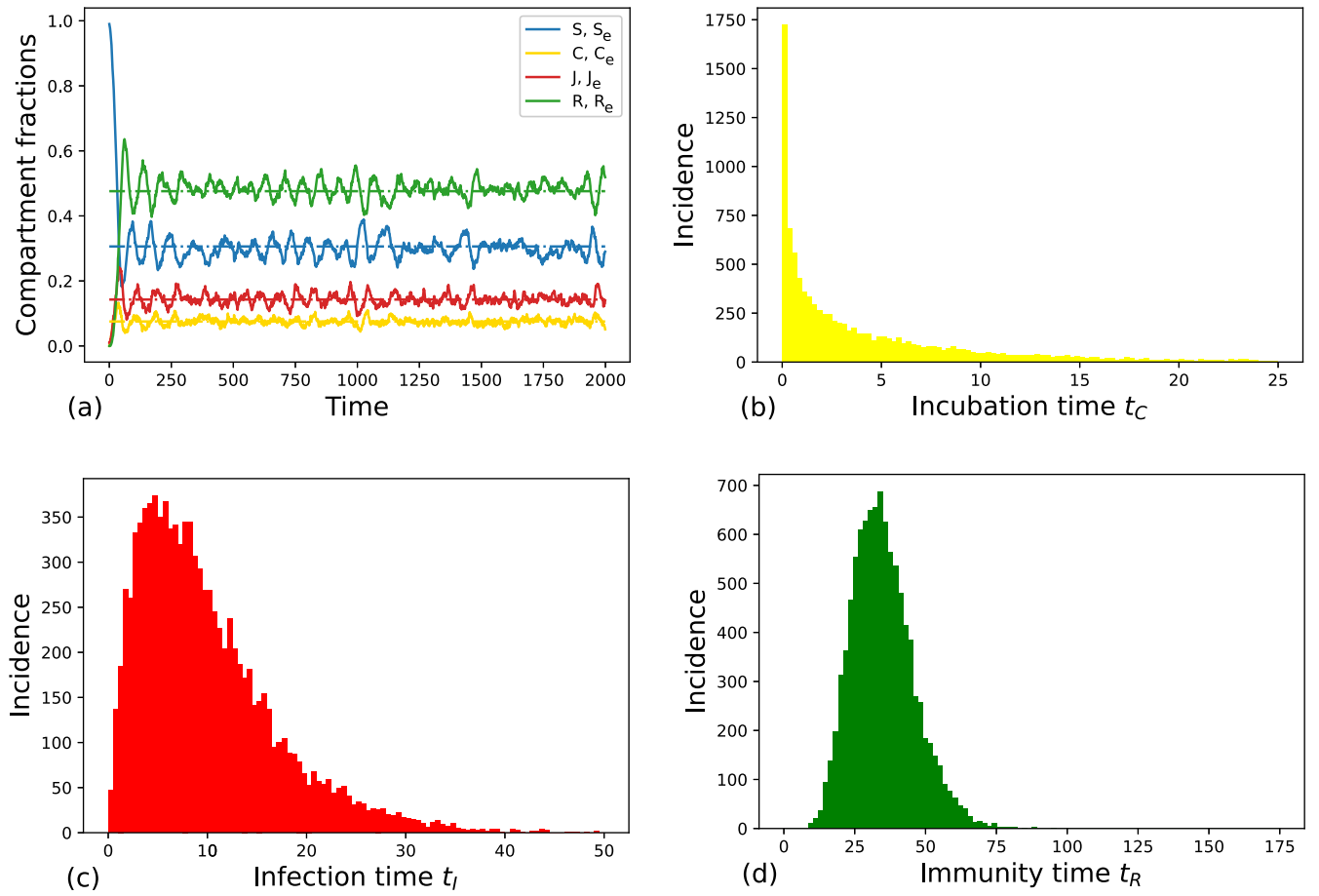

FIG. 4. Compartment fractions averaged over ten random-walk realizations with $Z = 100$, $N = 11$ (density $Z/N^2 \approx 0.83$), $P_{\text{inf}} = 0.9$, and Γ-distributed waiting times having the means $\langle t_C \rangle = 5$, $\langle t_I \rangle = 10$, $\langle t_R \rangle = 35$, $\xi_C = 0.1$, $\xi_I = 0.2$, and $\xi_R = 0.3$. By using Eq. (47) for the numerical evaluation we get (dashed lines) $S_e \approx 0.31$, $C_e \approx 0.075$, $J_e \approx 0.14$, and $R_e \approx 0.48$; with Eq. (48) we have $r_C \approx 1.08$, $r_I \approx 1.03$, and $r_R \approx 0.98$. We depict the corresponding Γ-distributed waiting times (b) t_C, (c) t_I, and (d) t_R with the parameters and color code used in the simulation of (a).

by employing the numerically determined S_e. In all simulations with existing endemic equilibria and sufficiently large observation time the ratios $r_{C,I,R} \approx 1 + O(10^{-2})$ are up to a few percent close to one, confirming impressively the prediction $C_e{:}J_e{:}R_e = \langle t_C \rangle{:}\langle t_I \rangle{:}\langle t_R \rangle$ of the macroscopic model (28). In the following discussion we give numerical evidence that our macroscopic *S-C-I-R-S* model is well suited to the microscopic random-walk approach.

In the experiment of Fig. 4 the waiting times are broadly scattered and distributed by Γ distributions of different parameters. For the chosen parameters the epidemic dynamics converges rapidly to the endemic states with the ratio $C_e{:}J_e{:}R_e = \langle t_C \rangle{:}\langle t_I \rangle{:}\langle t_R \rangle$ predicted by Eqs. (28). In Fig. 5 we have equal δ-distributed waiting times and very large R_0. The measures (48) are $r_{C,I,R} \approx (1.01, 1.00, 0.99)$ close to one and indicate excellent accordance with Eqs. (28), although the observation time is not very large. In this plot (blue dash-dotted line) S_e is slightly overestimated as (47) is an asymptotic relation holding for large t.

The depicted time evolutions of Fig. 6 exhibit for δ-distributed waiting times slightly attenuated oscillations. This indicates that this case is close to an oscillatory (Hopf) instability. We approach this instability by slightly reducing the walkers density (reducing R_0). The corresponding persistent oscillatory behavior is shown in Fig. 7(a).

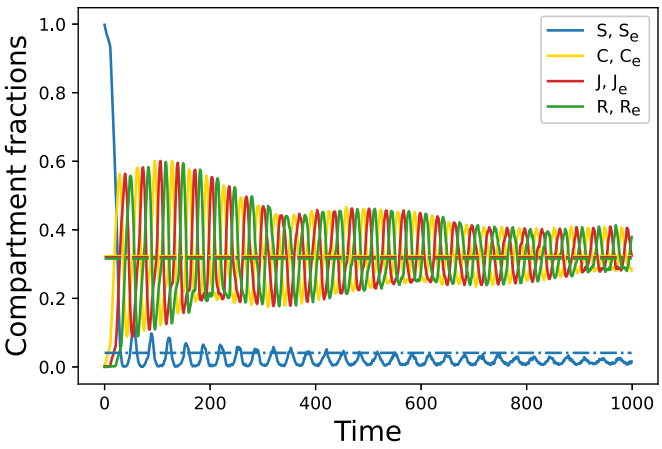

FIG. 5. (a) Average over five random-walk realizations and (δ-distributed) waiting times $t_C = t_I = t_R = 10$ ($T = 30$) with $Z = 500$, $N = 11$ (density $Z/N^2 \approx 4.13$), and $P_{\text{inf}} = 0.9$. We have small $S_e \approx 0.04$ ($R_0 \approx 24, 39$) and $C_e = J_e = R_e \approx 0.32 \approx \frac{1}{3}$ (dashed lines).

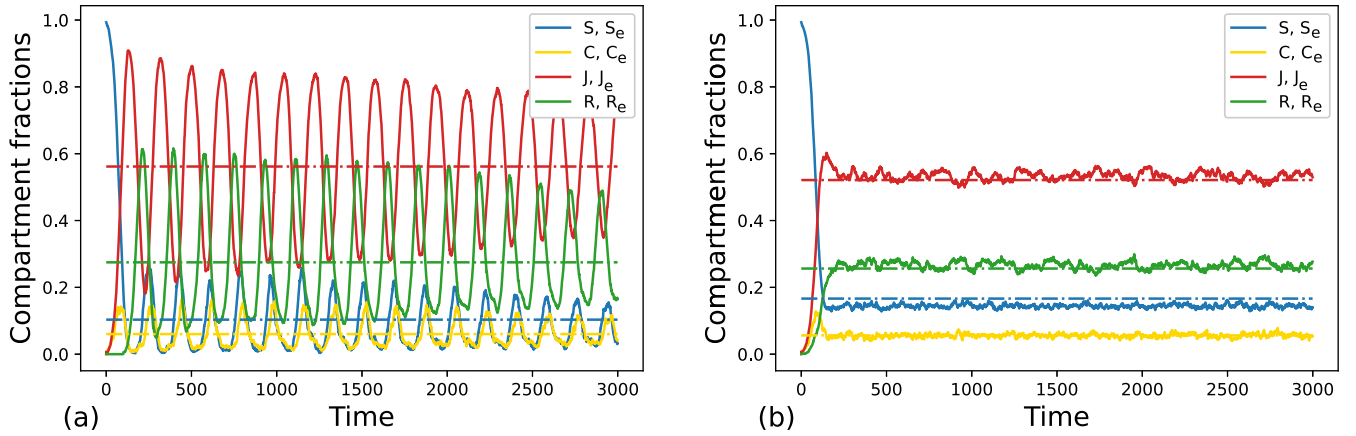

FIG. 6. Compartment fractions averaged over ten random-walk realizations for (a) δ-distributed and (b) exponentially distributed waiting times with $Z = 150$, $N = 21$ (density $Z/N^2 \approx 0.34$), $P_{\text{inf}} = 0.9$, and the means $\langle t_C \rangle = 10$, $\langle t_I \rangle = 100$, and $\langle t_R \rangle = 50$. (a) Endemic states (dash-dotted lines) for δ-distributed waiting times: $S_e \approx 0.10$ ($R_0 \approx 9.68$), $C_e \approx 0.06$, $J_e \approx 0.56$, and $R_e \approx 0.27$. The ratios are $r_C \approx 1.07$, $r_I \approx 1.00$, and $r_R = 0.98$ [see (48)]. (b) Endemic states (dash-dotted lines) for exponential waiting times: $S_e \approx 0.16$ ($R_0 \approx 6.01$), $C_e \approx 0.06$, $J_e \approx 0.52$, and $R_e \approx 0.26$. The ratios are $r_C \approx 1.07$, $r_I \approx 1.00$, and $r_R \approx 0.98$.

Figures 7(a) and 7(b) differ by changing to exponentially distributed t_C and Γ-distributed t_R. All other parameters including the density are identical in both Figs. 7(a) and 7(b). Figure 7(a) exhibits a Hopf unstable persistent oscillatory behavior. The resulting S_e in Fig. 7(b) is slightly lower, increasing R_0 and leading to attenuation of the Hopf oscillations. As both plots employ identical parameters but different waiting-time PDFs, this demonstrates that R_0 also depends on further characteristics such as the variance.

Figure 8 shows a numerical solution of the macroscopic system (30) for the same parameters as in Figs. 6(a) and 7(a). The at least qualitative similarity to the microscopic result is impressive [see in particular Fig. 7(b), which exhibits attenuated oscillations]. In both models the number of infectious individuals dominates due to the relatively long infection time. In the long-time limit the oscillations are damped and the endemic equilibrium is asymptotically reached.

In the simulations of Figs. 9 and 10 we consider various combinations of waiting-time distributions. In Fig. 10 we compare δ-distributed waiting times and Γ-distributed waiting times with the same means. In Fig. 10(a) r_C has a relatively large (by 15%) deviation from Eq. (28). This can be explained as (47) is an asymptotic relation converging for large t to the endemic values where in Fig. 10(a) the time range is not very large. In Fig. 10(b) the time range is considerably increased; thus all ratios $r_{C,I,R}$ become very close to one, indicating excellent accordance with Eq. (28). The slightly different absolute values are due to slightly different $R_0 = 1/S_e$ despite all parameters P_{inf}, Z, and N being identical. This confirms our observation in Fig. 7 that R_0 depends on further characteristics of the waiting-time PDFs such as their variances.

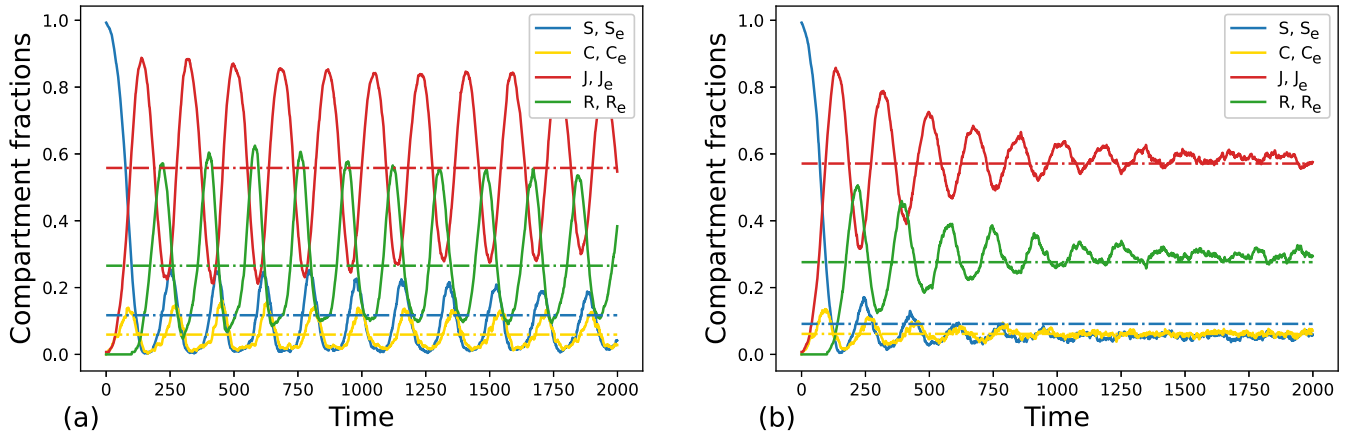

FIG. 7. (a) Plot of δ-distributed waiting times, with all parameters as in Fig. 6(a) but with $Z = 140$ to have a slightly lower density to approach the oscillatory (Hopf) instability (density $Z/N^2 \approx 0.32$). Endemic values are $S_e \approx 0.11$ ($R_0 \approx 8.53$), $C_e \approx 0.06$, $J_e \approx 0.56$, and $R_e \approx 0.26$ and the ratios are $r_C \approx 1.07$, $r_I \approx 1.01$, and $r_R \approx 0.96$. (b) Identical parameters (including density) as in (a) but with exponentially distributed t_C with $\langle t_C \rangle = 10$, Gamma-distributed t_R with $\xi_R = 0.1$ and $\langle t_R \rangle = 50$, and t_I is δ distributed ($t_I = 100$). The different types of distributions decrease slightly $S_e \approx 0.09$ with increasing $R_0 \approx 10.95$ compared to (a), leading to attenuated oscillations. The other endemic values are $C_e \approx 0.06$, $J_e \approx 0.57$, and $R_e \approx 0.28$ and the ratios are $r_C \approx 1.08$, $r_I \approx 1.00$, and $r_R \approx 0.97$.

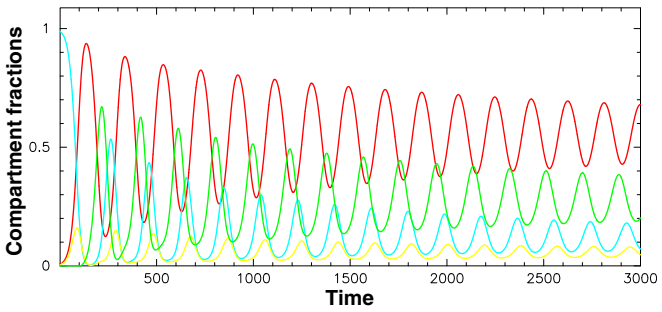

FIG. 8. Numerical solution of the ODE model (30) with the parameters of Fig. 6(a) and $R_0 = 9.1$, $j_0 = 0.01$, $s_0 = 0.99$, and $c_0 = r_0 = 0$. The color code is the same as in Fig. 6.

Figure 11 shows again the numerical solution of the macroscopic system (30) which is here for the smaller R_0, again in good agreement with the averaged microscopic behavior.

V. CONCLUSION

We have studied a macroscopic four-compartment *S-C-I-R-S* model with memory effects introduced by random compartmental waiting times. We derived evolution equations for different arbitrary waiting-time distributions and considered pertinent cases such as exponential (memoryless), Mittag-Leffler (fat-tailed with long memory), and sharp (δ-distributed) waiting times. We highlighted connections with general fractional calculus and showed that the evolution equations are of general (fractional) type [Eqs. (11) and (A1)]. For waiting-time PDFs with existing mean, we obtained exact formulas for the endemic equilibrium and conditions of its existence and identified the basic reproduction number $R_0 = \beta\langle t_I\rangle$ as a crucial parameter controlling whether or not a *S-C-I-R-S* epidemic starts to spread.

We also found (Appendix B) that the healthy state always is unstable if t_I has a fat-tailed PDF regardless of the distributions of $t_{C,R}$. In this case R_0 and $\langle t_I\rangle$ do not exist. We interpreted this instability by the occurrence of very long infectious periods t_I strongly boosting the epidemic spreading. Due to their general importance, the time-fractional cases call for further thorough investigation.

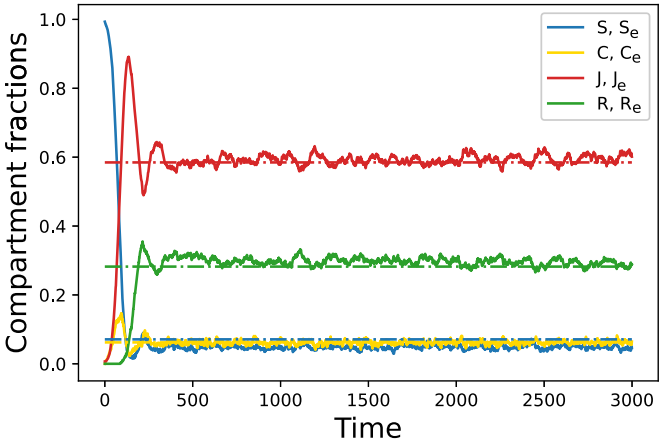

FIG. 9. Compartment fraction averaged over ten random-walk realizations and Gamma-distributed waiting times. The parameters are the same as in Fig. 6 except $\xi_C = 0.5$, $\xi_I = 0.2$, and $\xi_R = 0.01$, The endemic states (dashed lines) are $S_e \approx 0.07$ ($R_0 \approx 14.09$), $C_e \approx 0.06$, $J_e \approx 0.58$, and $R_e \approx 0.28$ and the ratios are $r_C \approx 1.06$, $r_I \approx 1.00$, and $R_R \approx 0.97$.

We compared the macroscopic *S-C-I-R-S* model with a random-walk approach. Our computer experiments have given numerical evidence that Eqs. (28) are fulfilled for any of the implemented waiting-time distributions (with initial conditions very close to the healthy state) whenever the endemic equilibrium exists. This was further confirmed by a comparison of results produced by the random-walk simulations and by direct numerical integration of Eqs. (30) for two cases of δ-distributed waiting times [see Figs. 6(a) and 8 and Figs. 10(a) and 11, respectively].

All these results give strong evidence that random walks offer an appropriate microscopic picture of the *S-C-I-R-S* dynamics. It was also found in the simulations that waiting-time PDFs with different variances but otherwise identical parameters may influence R_0.

For future research it would be desirable to relate the endemic value S_e, i.e., R_0 (here determined numerically), with characteristics of the waiting-time PDFs (such as their variances), infection probabilities in a collision of I and S walkers, and the random walk.

An interesting extension of our model could be considering the cases of a nonconstant total population, i.e., when we admit, on the one hand, birth and death rates (i). On the other hand, another promising direction would be to analyze how spatial inhomogeneities affect the epidemic dynamics (ii). In the first case (i) one can introduce a further compartment D (deaths) where a walker in state I can perform after a random waiting time t_I either a transition to R as in the present version of the model or a transition to D after a random waiting time t_D. The transition rate to D is the mortality rate due to the disease. The walkers having made a transition to R continue their transition pathway as in the present version of the model (i.e., to S and so forth). The choice whether a walker who is in compartment I performs a transition to D or R could be assumed random (with a certain probability) as well. Intuitively, one might expect that the cases of persistent oscillatory behavior in the infected population of the present version of the model would turn into attenuated oscillations.

Moreover, including spatial effects (ii) in the model leads to the occurrence of fluxes and inhomogeneities with macroscopic space-time partial differential evolution equations of general fractional types. The spatial effects involved are closely related to the assumption of admissible jumps of the walkers in their random walk, for instance, local steps as in the present model or long-range steps as in, for instance, Lévy flights [12] or a combination of both defining different classes of random walkers (corresponding to distinct mobility of individuals). It would be desirable to study the connection of the random walk (beyond simple walks) and the macroscopic space-time evolution equations. The present *S-C-I-R-S* model would represent a pertinent benchmark limiting case in the mentioned extensions (i) and (ii).

A further challenge is the investigation of microscopic random-walk models and their connection with oscillatory

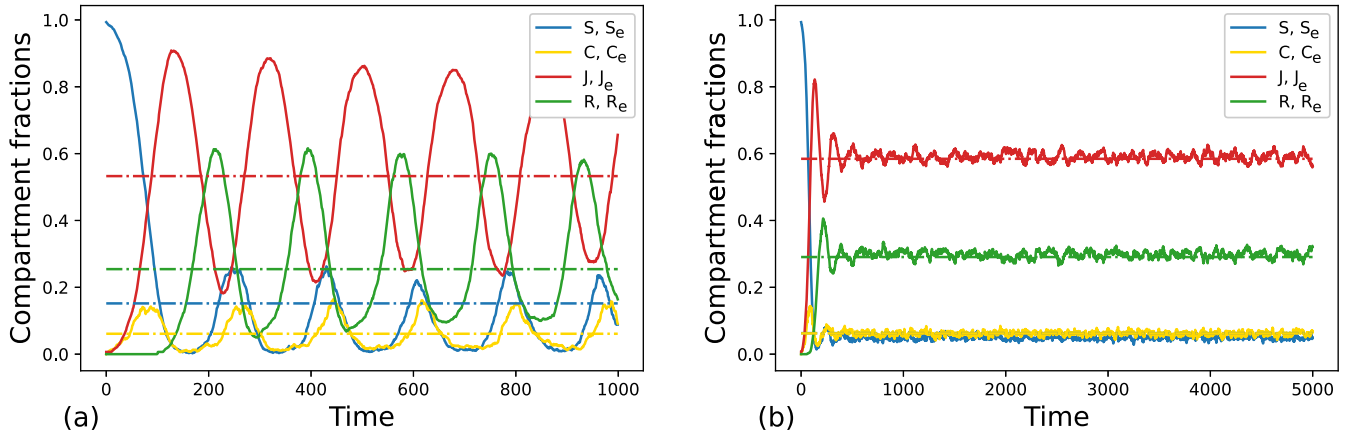

FIG. 10. (a) Plot of δ-distributed waiting times for the same parameters as in (b) except $\xi_{C,I,R} = 10^4$ [generating the δ distribution; see (45)]. The endemic values (dashed lines) are $S_e \approx 0.15$ ($R_0 = 1/S_e \approx 6.59$), $C_e \approx 0.06$, $J_e \approx 0.53$, and $R_e \approx 0.25$ with ratios $r_C \approx 1.15$, $r_I \approx 1.00$, and $r_R \approx 0.96$. (b) All waiting times are Γ distributed with their means identical to those of (a) with $\langle t_C \rangle = 10$, $\xi_C = 0.1$, $\langle t_I \rangle = 100$, $\xi_I = 0.1$ ($\alpha_I = 10$), $\langle t_R \rangle = 50$, $\xi_R = 0.05$, $Z = 150$, $N = 21$ (density $Z/N^2 \approx 0.34$), $P_{\rm inf} = 0.9$, $S_e \approx 0.06$ ($R_0 = 1/S_e \approx 15.91$), $C_e \approx 0.06$, $J_e \approx 0.58$, $R_e \approx 0.29$, and ratios $r_C \approx 1.06$, $r_I \approx 0.99$, and $r_R \approx 0.99$.

(Hopf) instabilities (condition for persistent oscillatory behavior). The characteristics of the Hopf instabilities of the healthy state and of quasiperiodic outbursts are closely related to the specific distributions and the mutual ratios of the waiting times $t_{C,I,R}$. Models of the *S-C-I-R-S* class as in the present paper may help decision makers to take improved protection measures such as confinement, wearing of masks, or vaccination. The effect of vaccination can be directly studied in our *S-C-I-R-S* model by considering the stability of initial states with a nonvanishing number of immune (vaccinated) individuals. We leave these issues for future research.

Generally, *S-C-I-R-S*–type models with memory as introduced in the present paper may open a wide research field to better understand the phenomenology of real-world epidemic dynamics.

ACKNOWLEDGMENTS

T.G. gratefully acknowledges to have been hosted at the Institut Jean le Rond d'Alembert for development of the PYTHON codes and participation in the present study. We thank the referees for useful comments, which helped us improve the presentation.

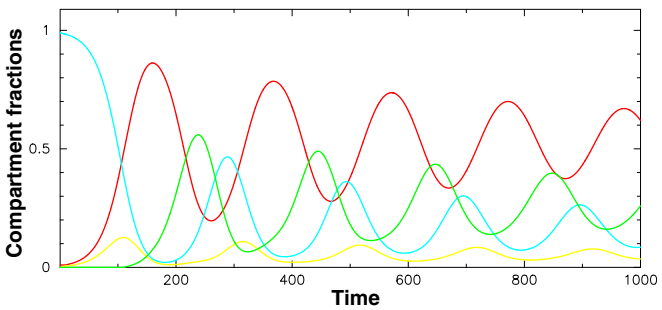

FIG. 11. Numerical solution of the ODE model (30) with the same parameters as in Fig. 10(a) and $R_0 = 6.6$, $j_0 = 0.01$, $s_0 = 0.99$, and $c_0 = r_0 = 0$.

APPENDIX A: GENERAL DERIVATIVES

We can alternatively represent Eqs. (11) in the Riemann-Liouville sense of general derivatives as

$$\begin{aligned}
\frac{d}{dt}s(t) &= -\mathcal{A}(t) + \frac{d}{dt}\int_0^t \mathcal{L}_R(t-\tau)r(\tau)d\tau,\\
\frac{d}{dt}c(t) &= \mathcal{A}(t) - \frac{d}{dt}\int_0^t \mathcal{L}_C(t-\tau)c(\tau)d\tau,\\
\frac{d}{dt}j(t) &= \frac{d}{dt}\int_0^t \mathcal{L}_C(t-\tau)c(\tau)d\tau\\
&\quad - \frac{d}{dt}\int_0^t \mathcal{L}_I(t-\tau)[j(\tau)-j_0]d\tau,\\
\frac{d}{dt}r(t) &= \frac{d}{dt}\int_0^t \mathcal{L}_I(t-\tau)[j(\tau)-j_0]d\tau\\
&\quad - \frac{d}{dt}\int_0^t \mathcal{L}_R(t-\tau)r(\tau)d\tau,
\end{aligned} \tag{A1}$$

which also are obtained straightforwardly from the Laplace transformed representation (9) and employing the definition (10). On the right-hand sides, general derivatives come into play. The notion of a general (fractional) derivative was introduced by Kochubei [29], generalizing $\frac{d}{dt}y(t)$ as (in the Caputo sense)

$$\begin{aligned}
D_t^* y(t) &= \int_0^t k(t-\tau)\frac{d}{d\tau}y(\tau)d\tau\\
&= \frac{d}{dt}\int_0^t k(t-\tau)y(\tau)d\tau - y_0 k(t) = D_t y(t) - y_0 k(t),
\end{aligned} \tag{A2}$$

with $y_0 = y(t)|_{t=0}$. The part $D_t y(t) = \frac{d}{dt}\int_0^t k(t-\tau)y(\tau)d\tau$ is a general derivative in the Riemann-Liouville sense for some admissible kernels $k(\tau)$ (see [29] for an outline of this theory). The general derivative (A2) has the LT

$$\int_0^\infty e^{-\lambda t} D_t^* y(t)dt = \lambda\hat{k}(\lambda)\hat{y}(\lambda) - y_0\hat{k}(\lambda). \tag{A3}$$

The general derivatives contain the class of standard fractional derivatives of Caputo and Riemann-Liouville type and for a $k(t) = \delta(t)$ the standard first-order derivative.

APPENDIX B: STABILITY ANALYSIS FOR ARBITRARY WAITING-TIME DENSITIES

In Sec. III we derived that the healthy state is unstable if $R_0 = \beta t_I > 1$ for δ-distributed kernels. Here we consider arbitrary waiting-time kernels first with finite means to generalize this result and at the end of this Appendix we briefly look at the time-fractional case. To this end we take into account that the PDFs $K_{C,I,R}(t)$ can be seen as a superposition (average over $t_{C,I,R}$) of the $\delta(t - t_{C,I,R})$ kernel as

$$K_{C,I,R}(t) = \langle \delta(t - t_{C,I,R}) \rangle = \int_0^\infty \delta(t-\tau) K_{C,I,R}(\tau) d\tau = (\delta \star K_{C,I,R})(t) \quad \text{(B1)}$$

and in this way we can average

$$\langle f(t_{C,I,R}) \rangle = \int_0^\infty K_{C,I,R}(\tau) f(\tau) d\tau \quad \text{(B2)}$$

for sufficiently good functions f and thus

$$\langle e^{-\mu t_{C,I,R}} \rangle = \hat{K}_{C,I,R}(\mu), \quad \text{(B3)}$$

yielding the Laplace transform of the PDF. Therefore, averaging Eqs. (30) for δ kernels over the waiting times $t_{C,I,R}$ brings us back to the general *S-C-I-R-S* equations (1), which can be seen from

$$\langle \mathcal{A}(t - t_C) \rangle = \int_0^t \mathcal{A}(t-\tau) K_c(\tau) d\tau = (K_C \star \mathcal{A})(t), \quad \text{(B4)}$$

where we used causality of $\mathcal{A}$ and K_C. Hence we can generalize the case of δ kernels (34) to any kernels by accounting for

$$\langle e^{-\mu(t_I + t_R + t_C)} \rangle = \hat{K}_C(\mu) \hat{K}_I(\mu) \hat{K}_R(\mu),$$

where we always use the mutually independence of the waiting times. Hence, by averaging Eq. (34) we get

$$\begin{aligned} A_0(u,w)[1 - \hat{K}_C(\mu)\hat{K}_I(\mu)\hat{K}_R(\mu)] + \mu u &= 0, \\ A_0(u,w)[1 - \hat{K}_C(\mu)] - \mu v &= 0, \\ A_0(u,w)\hat{K}_C(\mu)[1 - \hat{K}_I(\mu)] - \mu w &= 0, \\ A_0(u,w)\hat{K}_C(\mu)\hat{K}_I(\mu)[1 - \hat{K}_R(\mu)] - x\mu &= 0, \end{aligned} \quad \text{(B5)}$$

leading to the solvability condition

$$\begin{Vmatrix} \beta J_e[1 - \hat{K}_C(\mu)\hat{K}_I(\mu)\hat{K}_R(\mu)] + \mu & \beta S_e[1 - \hat{K}_C(\mu)\hat{K}_I(\mu)\hat{K}_R(\mu)] \\ \beta J_e \hat{K}_C(\mu)[1 - \hat{K}_I(\mu)] & \beta S_e \hat{K}_C(\mu)[1 - \hat{K}_I(\mu)] - \mu \end{Vmatrix} \mu^2 = 0. \quad \text{(B6)}$$

We have again [as in (35)] $\mu = 0$ as a threefold eigenvalue. The remaining nonzero eigenvalue is determined by

$$\mu = \beta S_e \hat{K}_C(\mu)[1 - \hat{K}_I(\mu)] - \beta J_e[1 - \hat{K}_C(\mu)\hat{K}_I(\mu)\hat{K}_R(\mu)]. \quad \text{(B7)}$$

We have to point out that in order to obtain these results we have relaxed causality in the exponential ansatz (33) and assumed that it is defined for all $t \in \mathbb{R}$. The difference of causal and noncausal averaging can be seen by comparing

$$\begin{aligned} \langle e^{\mu(t-t_C)} \rangle &= e^{\mu t} \int_0^\infty e^{-\mu\tau} K_C(\tau) d\tau = e^{\mu t} \hat{K}_C(\mu) \\ &\neq \langle \Theta(t - t_C) e^{\mu(t-t_C)} \rangle = e^{\mu t} \int_0^t e^{-\mu\tau} K_C(\tau) d\tau, \end{aligned} \quad \text{(B8)}$$

where $\Theta(\tau)$ indicates the Heaviside unit step function and corresponds to causality. To obtain the condition (B6) we have averaged as in the first line of (B8), where the exponential is noncausal, allowing exponentials with arguments $t - t_C < 0$ to contribute. Both sides become asymptotically equal in the limit $t \to \infty$. Hence, the relation (B6) can also be interpreted as the large-time asymptotics of causal averaging.

Let us focus now on the stability of the healthy state $s_0 = 1$. Then (B7) yields ($S_e \to s_0 = 1$ and $J_e \to j_0 = 0$)

$$\mu = \beta \hat{K}_C(\mu)[1 - \hat{K}_I(\mu)] = G(\mu). \quad \text{(B9)}$$

As in the case of δ-distributed waiting times, $G(\mu)$ is a concave function with $G(\mu) \to 0$ as $\mu \to \infty$; thus we can argue in the same way [see Eq. (37) and Fig. 2]. Hence there is an intersection $\mu_0 > 0$ only if $\frac{d}{d\mu} G(\mu)|_{\mu=0} > 1$. Expanding $G(\mu)$ (assuming existing mean $\langle t_I \rangle$) gives

$$G(\mu) = \beta[1 - \langle t_C \rangle \mu + o(\mu)] \langle t_I \rangle \mu = \beta \langle t_I \rangle \mu + o(\mu). \quad \text{(B10)}$$

Therefore,

$$\left. \frac{d}{d\mu} G(\mu) \right|_{\mu=0} =: R_0 = \beta \langle t_I \rangle > 1 \quad \text{(B11)}$$

is the condition for this instability of the healthy state and hence the interpretation as the basic reproduction number R_0 makes sense. This holds for waiting-time PDFs with existing means. On the other hand, the relation (B9) holds for any waiting-time PDF including fat-tailed ones, which we briefly consider in the following.

Time fractional case. Assuming $K_I(t)$ is a fat-tailed PDF such as the Mittag-Leffler PDF with $\hat{K}_I(\mu) = \frac{\xi_I}{\xi_I + \mu^\nu}$, $\nu \in (0, 1)$, and whether or not the other kernels have existing means we get, for $G(\mu)$,

$$G(\mu) = \frac{\beta}{\xi_I} \mu^\nu + o(\mu^\nu) > \mu \quad (\mu \to 0), \quad \text{(B12)}$$

where $o(\mu^\nu)$ indicates orders higher than ν. Thus (B9) (independent of $\frac{\beta}{\xi_I}$) always has a positive intersection since

$\nu \in (0, 1)$. We conclude that for fat-tailed $K_I(t)$ the healthy state always is unstable regardless of the distributions of t_C and t_R. Physically, this instability can be understood by the occurrence of very long infectious times t_I strongly boosting the epidemic spreading (corresponding to the limit $R_0, \langle t_I \rangle \to \infty$).

[1] W. O. Kermack and A. G. McKendrick, A contribution to the mathematical theory of epidemics, Proc. R. Soc. London A **115**, 700 (1927).

[2] R. M. Anderson, and R. M. May, *Infectious Diseases in Humans* (Oxford University Press, Oxford, 1992).

[3] M. Martcheva, *An Introduction to Mathematical Epidemiology* (Springer, Berlin, 2015).

[4] V. Belik, T. Geisel, and D. Brockmann, Recurrent host mobility in spatial epidemics: Beyond reaction-diffusion, Eur. Phys. J. B **84**, 579 (2011).

[5] L. Feng, Q. Zhao, and C. Zhou, Epidemic spreading in heterogeneous networks with recurrent mobility patterns, Phys. Rev. E **102**, 022306 (2020).

[6] A.-L. Barabási, *Network Science* (Cambridge University Press, Cambridge, 2016).

[7] R. Pastor-Satorras and A. Vespignani, Epidemic dynamics and endemic states in complex networks, Phys. Rev. E **63**, 066117 (2001).

[8] A. P. Riascos and J. L. Mateos, Random walks on weighted networks: A survey of local and non-local dynamics, J. Complex Netw. **9**, cnab032 (2021).

[9] T. Michelitsch, A. P. Riascos, B. A. Collet, A. Nowakowski, and F. Nicolleau, *Fractional Dynamics on Networks and Lattices* (ISTE-Wiley, London, 2019).

[10] M. Bestehorn, A. P. Riascos, T. M. Michelitsch, and B. A. Collet, A Markovian random walk model of epidemic spreading, Continuum Mech. Thermodyn. **33**, 1207 (2021).

[11] M. Bestehorn, T. M. Michelitsch, B. A. Collet, A. P. Riascos, and A. F. Nowakowski, Simple model of epidemic dynamics with memory effects, Phys. Rev. E **105**, 024205 (2022).

[12] R. Metzler and J. Klafter, The random walk's guide to anomalous diffusion: A fractional dynamics approach, Phys. Rep. **339**, 1 (2000).

[13] T. Sandev, R. Metzler, and A. Chechkin, From continuous time random walks to the generalized diffusion equation, Fract. Calc. Appl. Anal. **21**, 10 (2018).

[14] F. Mainardi, R. Gorenflo, and E. Scalas, A fractional generalization of the Poisson processes, Vietnam J. Math. **32**, 53 (2004).

[15] T. M. Michelitsch, F. Polito, and A. P. Riascos, Biased continuous-time random walks with Mittag-Leffler jumps, Fractal Fract. **4**, 51 (2020).

[16] T. M. Michelitsch and A. P. Riascos, Generalized fractional Poisson process and related stochastic dynamics, Fract. Calc. Appl. Anal. **23**, 656 (2020).

[17] H. E. Soper, The interpretation of periodicity in disease prevalence, J. R. Stat. Soc. **92**, 34 (1929).

[18] D. Faranda, I. P. Castillo, O. Hulme, A. Jezequel, J. S. W. Lamb, Y. Sato, and E. L. Thompson, Asymptotic estimates of SARS-CoV-2 infection counts and their sensitivity to stochastic perturbation, Chaos **30**, 051107 (2020).

[19] P. Manfredi and E. Salinelli, Population-induced oscillations in blended SI-SEI epidemiological models, Math. Med. Biol. **19**, 95 (2002).

[20] H. C. Tijms, *A First Course in Stochastic Models* (Wiley, New York, 2003).

[21] A. J. Lotka, *Analytical Theory of Biological Populations* (Plenum, New York, 1998).

[22] F. A. Rihan, *Delay Differential Equations and Applications to Biology* (Springer, Singapore, 2021).

[23] G. E. Hutchinson, Circular causal systems in ecology, Ann. N.Y. Acad. Sci. **50**, 221 (1948).

[24] D. Mackey and L. Glass, Oscillations and chaos in physiological control systems, Science **197**, 287 (1977).

[25] M. Bestehorn, E. V. Grigorieva, and S. A. Kaschenko, Spatio-temporal structures in a model with delay and diffusion, Phys. Rev. E **70**, 026202 (2004).

[26] L. Basnarkov, I. Tomovski, T. Sandev, and L. Kocarev, Non-Markovian SIR epidemic spreading model of COVID-19, Chaos, Solitons Fractals **160**, 112286 (2022).

[27] M. Bestehorn, *Computational Physics*, 2nd ed. (De Gruyter, Berlin, 2023).

[28] T. M. Michelitsch, F. Polito, and A. P. Riascos, On discrete time Prabhakar-generalized fractional Poisson processes and related stochastic dynamics, Physica A **565**, 125541 (2021).

[29] A. N. Kochubei, General fractional calculus, evolution equations and renewal processes, Integr. Equ. Oper. Theory **71**, 583 (2011).

[30] S. G. Samko, A. A. Kilbas, and O. I. Marichev, *Fractional Integrals and Derivatives: Theory and Applications* (Gordon and Breach, London, 1993).

[31] https://sites.google.com/view/scirs-model-supplementaries/accueil.

[32] W. Feller, *An Introduction to Probability and Its Applications*, 3rd ed. (Wiley, New York, 1968), Vol. 1.